Novel Application of Potentiometric Microelectrodes: Scanning Potentiometric Microscopy

Klára Tóth,[+] *Géza Nagy,*[+] *Chang Wei,*[++] and *Allen J. Bard*[++]

[+] Research Group for Technical Analytical Chemistry of the Hungarian Academy of Sciences, Institute for General and Analytical Chemistry, Technical University of Budapest, H-1111 Budapest, Hungary
[++] Department of Chemistry and Biochemistry, The University of Texas at Austin, Austin, TX 78712, USA

Received: February 22, 1995
Final version: April 3, 1995

Abstract
The techniques for the fabrication of a new type of potentiometric scanning electrochemical microscopic tip are described. Ion-concentration profiles generated in electrochemical model experiments, by enzyme catalyzed reaction and corrosion processes, as well as by the electrochemical reduction of zinc ions, have been studied and followed with micropipet ion-selective electrode based probe microscopy. Efforts devoted to developing methods to measure scanning tip-to-target distances are surveyed.

Keywords: Micropipet ion-selective electrodes, Zinc microelectrode, Scanning electrochemical microscopy

1. Introduction

The preparation, investigation and application of microelectrodes have been of interest in recent electroanalytical chemistry studies in which efforts have been devoted towards the reduction of the tip size of these sensors. The ultramicroelectrodes have a tip size so small that it is hard to imagine any further significant step in the direction of size reduction. Fabrication procedures reported for voltammetric disk electrodes show diameters of a few hundred nanometers [1], in contrast to micropipet type ion-selective electrodes that may have tip diameter of several tens of nanometers [2].

The introduction of submicron-sized ion-selective electrodes preceded the appearance of submicron voltammetric electrodes by decades. The first major steps in the development of ion-selective microelectrodes were made by experimental life scientists [3,4]. They, working more or less independently and often without any consultation with electrochemists, had a marked influence on the design of micro ion-selective electrodes. With good experience in micropipet preparation, they developed an universal type of micropipet ion-selective electrode. These microelectrodes, especially the double or multi-barrel versions, gained widescale application in the life sciences field. The micropipet ion-selective electrodes of high selectivity, however, only became available after the contribution of certain electroanalytical chemists, namely Professor Wilhelm Simon and his research school, who proved that designed, electrically neutral ligands [2,5,6] can be successfully employed in micropipet electrode fabrication. Based on their work, "ion-selective cocktails" became available for micropipet-type microelectrodes.

In life science experiments, microelectrodes are used to collect information on the local activity or concentration of different ions or molecules in the living object. Reduction of the size of the electrode yields a higher spatial resolution and less invasion of the organism.

In the early 1980s, a new kind of microscopy using an ultramicro measuring tip was developed based on the work of Binnig and Rohrer [7,8]. While most of the microscopic techniques rely on the interaction of electromagnetic waves with the target, this new microscopic technique is based on a different working principle. Here a sharp measuring tip is scanned over the target in close proximity (Z coordinate) with the help of a high precision positioner on the XY plane. The interaction between the measuring tip and the target of a different nature yields the signal. The intensities of the local signals corresponding to X, Y and Z location vectors are stored in a computer, and the data collected can be displayed as either a three-dimensional or a map-like color coded image of the target surface. This new technique is generally called scanning probe microscopy. Scanning tunneling microscopy (STM) and atomic force microscopy (AFM) were the first of these new types of image forming-techniques.

The high resolution of STM and AFM led to efforts to exploit existing electrochemical microelectrodes in probe microscopy. After the pioneering investigations by Engström et al. [9], Engström and Pharr [10], and Bard et al. [11] with ultramicro voltammetric electrodes, a new microscopic technique called scanning electrochemical microscopy (SECM) was invented and extensively exploited [11–18]. Detailed reviews discuss the principle, possibilities, and limitations of this technique [17,19,20].

SECM methods can be divided into two groups: methods using an active measuring tip, and methods using a passive measuring tip. In SECM with active measuring probes, i.e., voltammetric or amperometric tips, the measuring cell incorporates the target and a solution containing an electroactive species and the background electrolyte. The voltammetric current at a constant tip potential corresponding to the limiting current region is recorded while scanning the tip over the target. Once the ultramicroprobe electrode is far from the target surface, the tip current has a constant value. As the tip approaches an insulating surface, the current will decrease because the proximity of the surface hinders diffusion of the electroactive material. This effect is called "negative feedback". In contrast, an increase of the current can be observed when the active tip comes close to a conductive surface, if the conductive surface can regenerate the electroactive species used up in the electrochemical reaction, thus increasing its local concentration. This is called "positive feedback". SECM with an active measuring tip has the advantage that it can be used to image conducting as well as nonconducting surfaces. The image thus has topographic as well as chemical information.

The use of a passive measuring tip, i.e., an ion-selective electrode, in SECM is quite different. The tip does not generate a species to react with the target, and the tip potential is related to the local concentration of a chemical species. Thus, an image of a chemical nature can be obtained with a selective, passive

 © *VCH Verlagsgesellschaft mbH, D-69469 Weinheim, 1995* *1040-0397/95/0909-801 $ 5.00+.25/0*

measuring tip if the target generates a steady-state concentration profile. This means that a passive tip can best be used in SECM if a steady-state reaction proceeds on the target surface.

Most SECM work has employed an active measuring tip in the amperometric operation mode. However, certain systems (e.g., alkaline and alkaline earth metal or ammonium ion profiles) are inaccessible to the amperometric technique, but can be studied using passive, ion-selective tips. This is the main advantage of ion-selective electrodes as passive tips, in addition to the high selectivity of the potentiometric signal. Simultaneous imaging with active amperometric as well as ion-selective tips may provide additional information about the surface properties.

Several types of potentiometric tips have been prepared for scanning electrochemical microscopic studies. Silver and silver/silver chloride microdisk electrodes of 10 and 50 μm diameters were used [21] in SECM to probe silver and chloride ion fluxes during the electrochemical reduction and stripping of silver ions, as well as to monitor the chloride ion release and uptake of polyaniline during controlled potential experiments. For imaging local pH changes in several model chemical systems with SECM, antimony-based microdisk pH-sensitive electrodes were fabricated and used [22]. However, in order to extend the scope of the use of potentiometric SECM, it was a logical step forward to attempt to introduce micropipet type ion-selective electrodes in probe microscopy, since the fabrication procedure of micropipet electrodes which are selective to different ions is technically quite similar, and the tip size of this type of electrode is the smallest among micro ion-selective sensors available today.

Similarities can be found between the use of micropipet-type ion-selective electrodes in probe microscopy and in in vivo experiments when the aim of the experiment in the latter case is the determination of the local ion activity distribution in living objects. That measurement may be termed "one dimensional" microscopy, since the electrode penetrates axially step-by-step into the object, and the electrode potential is measured at different locations. One dimensional chemical images are often constructed in this way.

However, when passive measuring tips are employed in SECM, a method different from that with an amperometric tip is required for the measurement of the absolute tip-to-target distance. Without exact knowledge of the position of the tip over the target, no exact quantitative information can be obtained about the concentration profile near the target surface, and an accidental "crash" of the delicate tip on the target often results in tip damage. It is not easy to find an appropriate tip-to-target distance measuring method. In some cases optical microscopy can be used, but it is not usually practical with micropipet tips of micrometer scale.

In our work efforts have been devoted to determine different electrochemical methods and tips for tip-to-target distance measurements in potentiometric SECM. In this article, we compare these different approaches and report on the capabilities and limitations of the individual methods. The scope of potentiometric SECM is demonstrated by imaging targets of different origin. Moreover, the fabrication and the analytically important parameters of a new, ionophore-based zinc micropipet electrode and its potential use in potentiometric SECM are demonstrated.

2. Electrochemical Tip–Target Distance Calibration in Potentiometric SECM

Three different approaches have been elaborated in our work on distance measurements in potentiometric probe microscopy [22, 23]. In the following, these approaches are surveyed and briefly discussed.

2.1. Distance Measurement Using a Double Function Antimony Microdisk Electrode

Many heterogeneous chemical reactions involve local pH changes. Antimony electrodes are often used as pH sensors instead of pH glass electrodes, especially in applications where, due to safety reasons, glass electrode measurements are not recommended (e.g., in the food industry). Well-functioning, miniaturized antimony electrodes with good dynamic response characteristics have been reported previously [24–26]. It was expected, therefore, that antimony microdisk electrodes could be used advantageously as measuring tips for pH profile based potentiometric imaging. However, antimony working electrodes have not found applications in voltammetric practice. Neither the applicable potential window nor the chemical stability of the antimony electrode surface can match the relevant properties of the generally used voltammetric working electrodes. A question arose, however, as to whether an antimony electrode could be employed as a measuring tip in amperometric SECM. As a matter of fact, in amperometric scanning electrochemical microscopy, any electrode material can be employed that provides a stable, concentration-dependent signal at the working electrode potential in the solution media selected. Since quite a few reversible redox couples are available for electrochemical microscopy, we tested the antimony electrode as an amperometric electrode. Preliminary experiments were carried out in our laboratory with conventional-sized antimony electrodes, which proved that a stable amperometric response could be obtained for several electroactive molecules. This validated the idea that a double function antimony measuring tip could be made for SECM too.

In our work, a micro antimony electrode functioned well in both amperometric and potentiometric operation modes, and the tip–target distance could be measured in the amperometric mode. This was done by recording the quasi-reversible oxygen reduction current while the electrode aproached the target surface. The absolute tip-target distance was determined [22] by fitting the measured data to the theoretically derived and experimentally well-proven equation for the approach curve in reference [19]. For this SECM study a new type of shielded microdisk antimony electrode was fabricated; its applicability in pH profile based potentiometric SECM has been investigated [22,27].

2.2. Distance Measurement with an Amperometric Auxiliary Metal Electrode Barrel

The development of an appropriate micropipet-type measuring tip for SECM would be a universal solution for the potentiometric detection of different ions, because by changing the "measuring cocktail", different ion-selectivity can be achieved. The double-barrel version micropipet electrodes are also popular in in vivo life science measurements. Thus, we investigated the applicability of this type of tip in microscopy. Our intention was to use one of the barrels for distance measurement and the other for selective potentiometric imaging. The distance-measuring barrel can be a shielded amperometric microdisk electrode attached to the potentiometric micropipet barrel. However, the preparation of a double-channel measuring tip with the necessary configuration on a

micrometer scale is very difficult. Attempts at pulling double-barrel pipets with platinum, gold, or silver wires, or carbon fiber inserted previously in one of the barrels were not successful; these efforts always resulted in distorted, asymmetric pipets. Therefore another approach was tried. One of the barrels of the ready-made double-barrel pipets was converted into an amperometric microdisk electrode by filling the interior of the barrel with a metal of low melting point. Since mercury does not "wet" the glass, it retreats from the tip and therefore cannot be used. However, by filling one of the barrels of the micropipet with gallium, microdisk electrodes applicable for amperometric distance measurements could be prepared [28]. Gallium has a melting point of 28.9°C and tends to remain in an overcooled liquid state under ambient laboratory conditions after it has been melted. Like antimony, gallium metal is not a really good voltammetric working electrode surface [29]. However, there are several electrochemically active materials which can be used for amperometric imaging or tip–target distance measurement with gallium microdisk electrodes in the amperometric operation mode. In our studies, the applicability of the gallium microdisk electrode as an amperometric SECM tip has been proven for distance measurements and for imaging different targets.

2.3. Distance Measurement with an Open Micropipet Auxiliary Barrel

In conductance microscopy, the topographic imaging of targets is carried out with an open micropipet electrode tip [30, 31]. This validates the idea that the tip–target distance can be measured with a silver/silver chloride, sodium chloride open micropipette barrel attached to the potentiometric passive imaging micropipet tip in a double-barrel configuration. The theory of this mediatorless distance estimation technique has been elaborated, and the method was demonstrated in a recently published study [23].

To understand the working principle of this technique, let us consider the following. A constant dc voltage is applied between a conventional-sized silver/silver chloride electrode and the distance measuring silver/silver chloride within an open micropipet filled with 0.1 M sodium chloride. The current observed is due to the following reversible process occurring at the two electrode/solution interfaces

$$AgCl + e^- \rightleftharpoons Ag + Cl^- \quad (1)$$

Because both electrodes have large surface areas relative to the aperture in the micropipet tip and the charge transfer processes are rapid, the current is basically limited by the total solution resistance (R_t). R_t is the sum of the resistance of the internal solution of the micropipet tip and an external solution resistance: $R_t = R_{tip} + R_{sol}$. R_t may be calculated from the applied voltage and the measured current. As the tip approaches the target, R_{tip} is unchanged, but the electrode's aperture can block the diffusion of the ions and therefore cause the external solution resistance to increase, and the current to decrease. If index B refers to the bulk of the solution and L ($L = d/a$) to the dimensionless distance between the target and the tip (d is the tip–target distance and a is the tip radius) then

$$\frac{R_{t(B)}}{R_{t(L)}} = \frac{i_{t(L)}}{i_{t(B)}} \quad (2)$$

and

$$\Delta R_{(L)} = R_{t(L)} - R_{t(B)} \quad (3)$$

Then, using results of the amperometric approach curve [19]

$$\frac{\Delta R_{(L)}}{(R_t - R_{tip})} = -0.708 + \left(\frac{1.515}{L}\right) + 0.6553 \exp\left(\frac{-2.4035}{L}\right) \quad (4)$$

where R_{tip} is the solution resistance inside the micropipet, which is independent of the distance L.

The resistance R_t can be calculated from the potential and the current (i) and the equation $R_{t(B)} = R_t - R_{tip} = 1/(4\kappa a)$ where κ and a are the specific resistance of the solution and the radius of the aperture of the tip, respectively. $\Delta R_{(L)}$ is obtained experimentally, while the distance d can be determined from Equation 4 if the value of a is known. Since no faradaic electrode reaction can occur at the target surface, electrically conductive and isolating surfaces behave similarly.

The sensitivity of this distance measuring technique depends on the relative values of R_{tip} and $R_{t(B)}$. If $R_{tip} \gg R_{t(B)}$, then the distance change will not result in a significant change of the current.

3. Experimental

3.1. Reagents and Materials

The chemicals used in the experiments were of reagent grade or better. The ionophores and related compounds used for the ion-selective electrode preparation were obtained from Fluka, except for the Zn^{2+} ionophore, *N*-phenyl-iminodiacetic acid *N'*-*N'*-dicyclohexyl-bis-amide, which was synthesized as previously described [32]. Ag wire, Au wire, and Ga metal were purchased from Aldrich, Goodfellow, and Johnson Matthey (Seabrook, NH), respectively. Double and single barrel borosilicate glass capillary tubes were obtained from Shutter Instruments (Novato, CA) and WPI (Sarasota, FL).

3.2. Fabrication of the Microelectrodes

3.2.1. Antimony Microelectrode

The double function antimony electrode was prepared as described in reference [22]. The melted antimony metal was drawn into a thick walled capillary (inner diameter 1 mm, outer diameter 7 mm) with a 50 mL syringe. The capillaries were then manually pulled from the antimony filled tube. Antimony-filled capillaries that were about 5 cm long with 20–200 μm diameter antimony fibers were selected and pulled again using the heating coil of a commercial electrode puller (Stoelting). A small weight was attached to the end of the capillary and the voltage of an electric power supply connected to the heating coil was controlled continuously while observing the extension of the capillary. A short, tapered section of the capillary was cut to expose an antimony disk, and this was mounted in another glass capillary. Electrical contact was made with mercury and introduced through the supporting capillary. The ratio of the total tip diameter to the diameter of the antimony microdisk (RG) was typically from 5 to 10. The thick glass support allowed careful polishing of the antimony disk (Fig. 1a).

3.2.2. Gallium Filled Micropipet Electrodes

Gallium microdisk electrodes were fabricated from pulled glass capillaries with tips of micrometer dimensions. Gallium metal was melted in a small glass container in a water bath and then introduced into the glass capillary barrel from the back side with the aid of a syringe. The length of the gallium inside the

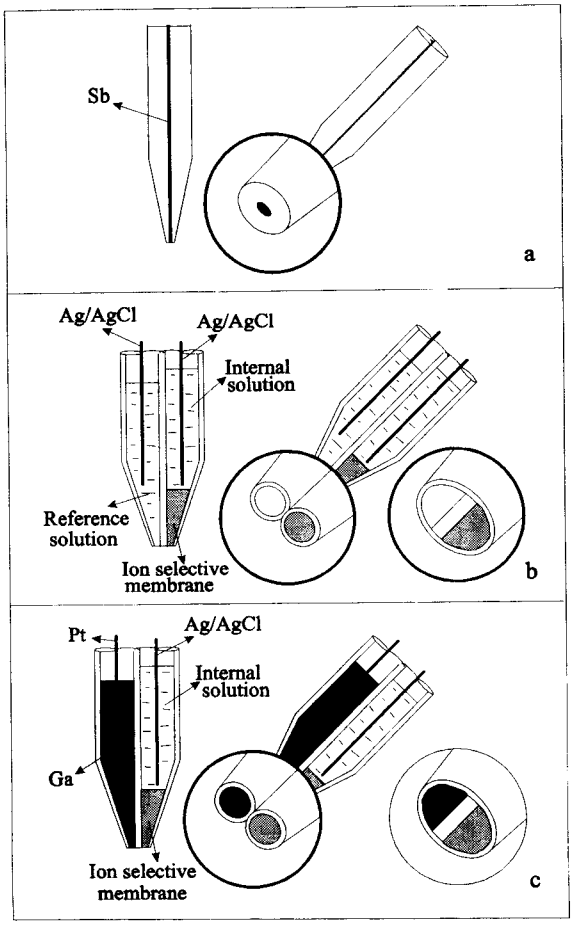

Fig.1. Schematic diagram of three types (a,b,c) of ion-selective microelectrodes used as SECM tips: a) antimony tip; b) dual-channel microelectrode with ISME (ion-selective membrane electrode) and Ag / AgCl micropipet electrode; c) dual-channel microelectrode; one channel with ion-selective membrane and the other with gallium.

barrel was about 2 cm. The gallium was then forced to the end of the tip by careful centrifuging. Periodically the centrifuging was stopped and the position of the gallium was checked under a microscope. Electrical contact was made by inserting a Pt wire into the gallium from the back. To solidify the gallium, the ready-made electrodes were kept in a refrigerator.

3.2.3. Ion-Selective Microelectrodes

Single and double-barrel ion-selective electrodes were made from borosilicate glass capillaries. In the case of double-barrel electrodes, the second barrel served for distance measurement. It was prepared with either a silver/silver chloride electrode or a Ga-microdisk electrode (Fig. 1b and c). Before pipet pulling, the glass tubes were soaked in a 1:1 (v/v) mixture of sulfuric acid and 30 % hydrogen peroxide for 24 h and then washed thoroughly with double-distilled water. They were dried at 120°C for about 30 min, just before pulling. A laser-based puller (Model P-2000, Sutter Instruments) and a conventional one (Stoelting) were used for micropipet fabrication. The micropipet barrels to be used for ion-selective electrode preparation were silanized with dimethyldichlorosilane vapor introduced by syringe injection. The silanization process was completed by allowing the glass surface to react with the vapor for 2 h at 120°C. In the case of double barrel electrodes, silanization of the distance measuring barrel was avoided by continuously flushing nitrogen gas through it during the ion-selective barrel silanization.The silanizing vapor was removed by suction and the ion-selective barrels were back-filled with the proper internal filling solution using a syringe. The tip of the ion-selective barrel was front filled with the corresponding ion-selective cocktail by capillary action and slight suction. A chlorinated silver wire was inserted to complete the ion-selective microelectrode half-cell.

Zinc and ammonium ion-selective microelectrodes were fabricated for SECM with ionophores such as *N*-phenyl-iminodiacetic acid *N'*-*N'*-dicyclohexyl-bis-amide (Zn^{2+}-ionophore, ligand 4 in reference [32]) and nonactin (NH_4^+-ionophore, Fluka, 09877). The ion-selective cocktail was prepared by dissolving 5–7 % (w/w) ionophore in 2-nitrophenyl octyl ether and adding 30–70 mol % potassium tetrakis (4-chlorophenyl) borate (KTpClPB) (relative to the ionophore). The internal filling solutions were 0.001 M $Zn(NO_3)_2$ and 0.1 M NH_4Cl, respectively.

3.3. Preparation of the Targets

Micropipet and inlaid microdisk type targets were prepared for the studies with an active surface area of 1–25 μm diameter. In one part of the experiments, dc current driven ionic migration and diffusion created a target concentration profile in the solution. In this case, the target was made of a U-shaped glass tube with a micropipet tip opening of 1–25 μm at one end. After completely filling the U-tube with a solution containing the ion of interest, the capillary end of the U-tube was inserted into the measuring cell through a hole in the center of the cell base. The cell contained a blank solution, i.e., a background electrolyte selected by considering the selectivity properties of the relevant ion-selective electrode. Two silver/silver chloride wires were placed in the noncapillary end of the U-tube and the bulk solution of the cell, respectively. These electrodes were connected with appropriate polarity to a dc current source.

The preparation of the inlaid microdisk immobilized enzyme targets has been described previously [22]. The micropipet type urease targets were made by dipping the micropipets of 5–10 μm diameter into 25 % glutaraldehyde solution while a small amount of the solution was drawn into the tip by capillary action. After about 10 min, the excess glutaraldehyde solution was sucked out and the enzyme solution (25 mg/ml urease) prepared with phosphate buffer (pH 7) was introduced into the tip. About 20 min crosslinking reaction time was allowed and the excess glutaraldehyde was removed by soaking the pipet tip in 10 mM asparagine solution. The enzyme target was then inserted into the base of the cell for the experiments.

For the electrodeposition of zinc, a microdisk gold amalgam electrode was used as a target. To prepare such a target, a 25-μm diameter gold wire was heat sealed in a glass tube under vacuum by conventional techniques. After polishing, the gold microdisk electrode was dipped into a mercury pool for a few seconds to allow the formation of amalgam on the Au surface. The excess mercury was wiped off and the electrode was inserted into the cell.

In all experiments an SECM cell made of Teflon was used. Its volume was about 4 mL.

3.4. Instrumentation

A block diagram of the SECM set-up, described in detail elsewhere, is shown in Figure 2 [22]. A CE-1000 micro positioning device (Burleigh Instruments, Fishers, NY) connected

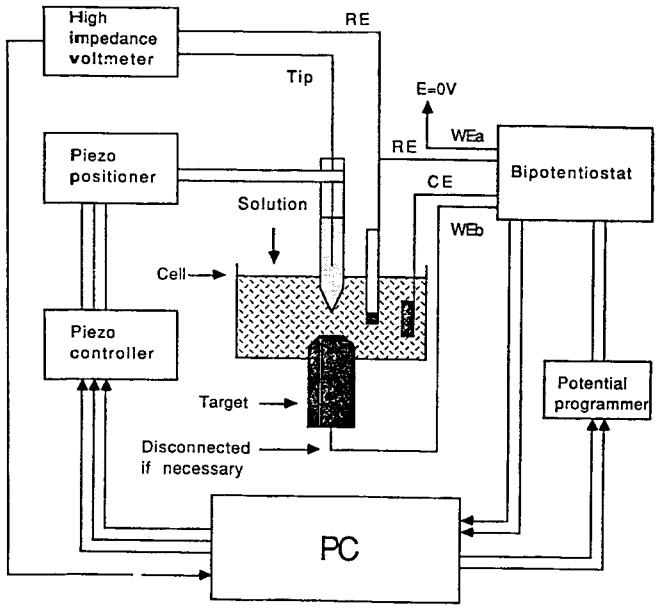

Fig. 2. Block diagram of the potentiometric SECM set-up. WE: working electrode; CE: counter electrode; RE: reference electrode.

to a PC (personal computer) was used to control the movement of three piezoelectric inchworm motors. The electrochemical cell with the target of interest placed in the middle of the cell base was mounted on a horizontal stage, and the microelectrode measuring tip was mounted on a three-axis translation stage that allowed submicron scale tip positioning. An EI-400 bipotentiostat (Ensman Instruments, Bloomington, IN) was used for potential control and current measurements, while the potentiometric measurements were made with a homemade high impedance voltmeter. An agar gel salt bridge with 0.01 M sodium chloride electrolyte was used to connect the reference electrode (RE) chamber to the cell. A BAS 100B electrochemical analyzer (BAS, West Lafayette, IN) was employed to perform the voltammetric measurements. For the electrochemical characterization of the micropipet ion-selective electrodes, a homemade high impedance voltmeter was used.

4. Results and Discussion

4.1. Measurements with a Double Function Antimony Electrode

As expected, the potentiometric pH response of the antimony microelectrodes in phosphate buffer of pH 5–9.5 was found to be linear with a slope of 40–50 mV/pH. This is typical for a polycrystalline antimony electrode. Surface oxidization by soaking the antimony in 0.1 M permanganate solution did not result in a noticeable increase in the pH sensitivity.

The cyclic voltammetric behavior of the antimony electrode in the presence of different electroactive species has been checked. The cyclic voltammograms of $Ru(NH_3)_6^{3+}$ as well as methyl viologen solutions also containing 0.1 M KCl were reproducible, and the peak current on an antimony microdisk electrode showed a concentration dependence. While approaching different target surfaces with the electrode in an amperometric operation mode, the positive and the negative feedback effects were observed, and the current–distance curves thus recorded were close to those predicted by the theory. Moreover, the electrochemical reduction of oxygen also provided reproducible voltammetric signals on antimony microelectrodes, and the steady-state oxygen reduction current recorded at an electrode potential set in the range of −0.7 to 1.1 V reflected the oxygen concentration in the solution. This could also be used for distance measurements. Owing to the irreversible nature of the oxygen reduction, the current only showed a negative feedback effect. The oxygen reduction current–distance curve, measured with a 4 μm diameter antimony microelectrode, fitted the theoretical curve, as shown in our earlier publication [22]. It is important to point out that the use of the oxygen reduction current for distance measurement is advantageous because it avoids the need to add an additional redox couple to the solution in the measuring cell, which may interfere with the potentiometric measuring tip.

SECM with a pH-sensitive tip has been employed to study corrosion processes at a silver iodide ion-selective membrane target and to image the pH profile around a microdisk Pt cathode on the electrochemical reduction of water in weakly buffered solution, as well as to detect local enzyme activities by monitoring pH changes due to the enzyme-catalyzed hydrolysis of urea and the metabolic activity of living microorganisms, e.g., yeast [22]. The SECM experiments were carried out with the double-function antimony microelectrode tip in the following way. First the measuring tip was roughly positioned over the target in an empty mesuring cell using a telescopic lens for observation. After an air saturated pH 7.0 phosphate buffer was introduced, the tip was operated in amperometric mode at −0.8 V. It approached the target surface by means of the Z piezo controller. Owing to the blocking of diffusion, the oxygen reduction current decreased as the electrode approached the target. By fitting the i–d data to the theoretical working curve, the absolute surface-to-target distance was determined. After this, the tip potential was set to 0.0 V for a few seconds to reoxidize the surface film on the antimony disk. This was essential for restoring the original pH function. When required, the solution in the cell was changed, then the potentiometric

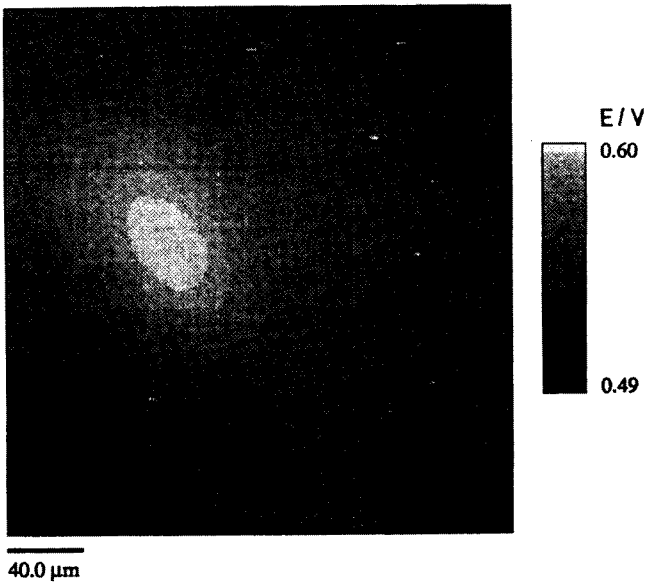

Fig. 3. Image of the pH profile on reducing water around a 25-μm Pt target in 0.1 M KCl and 1 mM phosphate buffer. The gray scale shows the antimony tip potential; the white corresponds to high pH. The potential of the target was -2 V vs. a platinum auxiliary electrode, the current was 0.5 μA. The tip diameter was 40 μm; the scan rate 10 μm/s; the tip-to-target surface distance was 33 μm.

operation mode was switched on. The pH profile over different areas of the target surface was investigated by moving the tip with the piezo controllers. pH profile images were recorded by scanning the tip in the $X-Y$ plane at a given distance from the surface.

A pH image over a Pt target reducing water is presented in Figure 3 as an example of SECM with an antimony tip. The Pt microdisk electrode of 25 μm diameter was connected as the cathode against a Pt auxiliary anode, and a reductive current of 0.5 μA was driven through the cell. As expected, the buffer capacity had a strong influence on the local pH profile. In this case, 1 mM phosphate buffer was employed as the background electrolyte and the antimony imaging tip of 40 μm diameter was placed at a distance of 33 μm above the target. The details of potentiometric SCEM with an antimony tip are given in references [22,27].

4.2. Measurements with a Double-Barrel Ion-Selective Measuring Tip

4.2.1. Amperometric Gallium Electrode SECM Tip

Preliminary experiments with gallium microdisk electrodes proved that reproducible voltammetric reduction waves can be obtained for $Ru(NH_3)_6Cl_3$ as an electroactive component. Figure 4 shows the cyclic voltammogram of a gallium microelectrode recorded in 0.1 M KCl solution containing 5 mM $Ru(NH_3)_6Cl_3$. By selecting the electrode potential more negative than −0.6 V, a stable, steady-state $Ru(NH_3)_6Cl_3$ concentration dependent amperometric current was recorded with a gallium microdisk electrode of double barrel configuration. The amperometric tip current was monitored while the electrode (double barrel configuration with a 22-μm gallium disk diameter) approached insulating (Teflon) and conductive (platinum) targets in a 0.1 M KCl background solution containing 5 mM $Ru(NH_3)_6Cl_3$ (Fig. 5). The current had a constant value when the electrode was far from the target

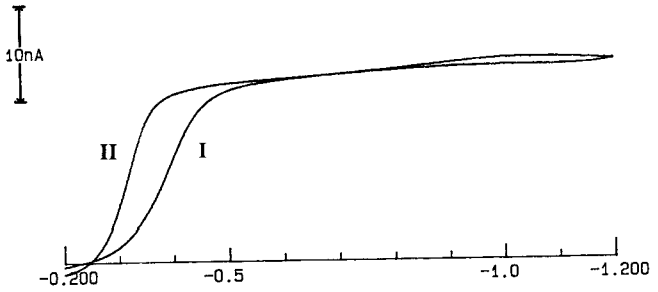

Fig. 4. Cyclic voltammogram of a 22-μm diameter gallium SECM tip in 5 mM $Ru(NH_3)_6Cl_3$ and 0.1 M KCl solution. A saturated calomel reference electrode was used, sweep rate = 5mV/s.

surface, but it increased in the proximity of a conducting surface (positive feedback) or decreased on approaching an insulating surface due to blocking of the analyte diffusion (negative feedback), as predicted by SCEM theory with a voltammetric tip. In Figure 5, the theoretical approaching curves (solid line) and the experimental data (the pluses) are exhibited showing fairly good agreement. The slight discrepancy between the experimental and the theoretical curves can be attributed to the geometry of the double-barrel configuration. It is worth mentioning that the gallium electrode tip in amperometric

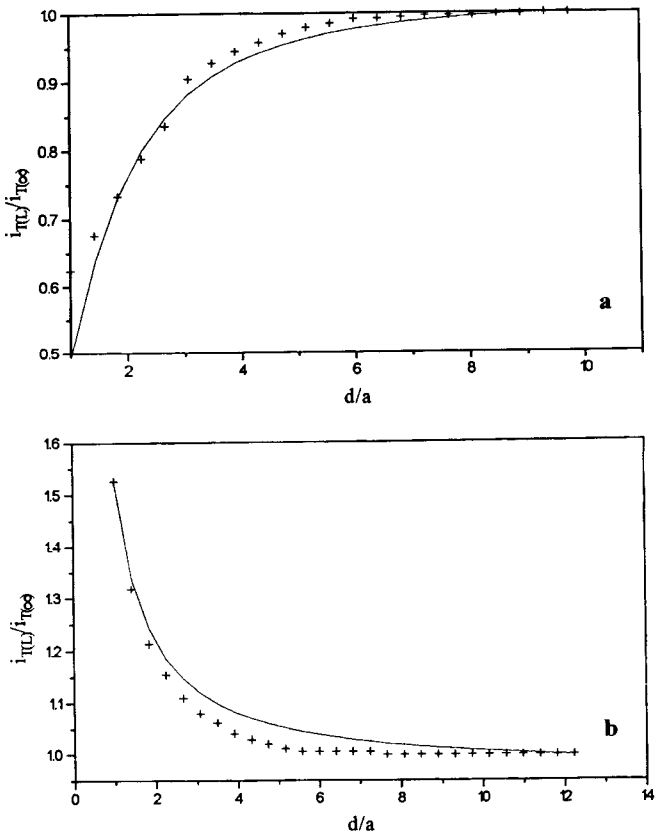

Fig. 5. Feedback current–distance curves for a gallium SECM tip of 22-μm diameter operating in amperometric mode in 0.1 M KCl and 5 mM $Ru(NH_3)_6Cl_3$: a) Pt surface, b) Teflon surface. Pluses represent experimental data, while the solid lines are theoretical data. The tip potential was held at -0.6 V vs. Ag/AgCl reference electrode.

operation mode in addition to the tip–target distance calibration can also be used for surface imaging.

The imaging with a double barrel (ISE and gallium) measuring tip was made in the following way. After rough positioning of the electrode over the target, 0.1 M potassium chloride solution containing 5 mM $Ru(NH_3)_6Cl_3$ was introduced into the cell and the tip–target distance was determined by fitting the experimental curve to the theoretical one. After this step, the solution in the cell was replaced and the potentiometric working mode activated. The ISE barrel was connected to the voltmeter and the tip was scanned in the $X-Y$ plane at a known distance Z from the surface.

It was experimentally proven that soaking different ion-selective electrodes in 5 mM $Ru(NH_3)_6Cl_3$ had no irreversible influence on the calibration properties of the ion-selective electrodes studied, as discussed later. The necessity of a redox mediator addition can be considered to be a disadvantage of the gallium SECM tip in a target distance measurement; however, there are experiments where double- (amperometric and potentiometric) imaging of the same surface can be very attractive.

4.2.2. Conductivity-Based Distance Measurement with an Open Micropipet Barrel in a Double-Barrel Configuration

Figure 6 shows an approach curve, i.e., the relative change of the solution resistance against tip–target distance for a silver/silver chloride micropipet electrode over a Teflon surface. The solid line represents the theoretical data, while the squares are the experimentally obtained data. The plot is constructed according to Equation 4. The resistance increases as the tip approaches the target surface indicating that the proximity of the target affects the current by blocking ion transport. The good fit of the measured data to the theoretical curve indicates that the open micropipet conductivity measurement can be used advantageously for tip–target distance measurements. A similar curve can be recorded for conducting surfaces, since the distance measurements are based on the very same, ion-transport blocking effect.

The main advantages of the conductivity based distance calibration are that it does not require an additional redox mediator and that the fabrication procedure of the double-barrel, ISE–open pipet measuring tip combination is well established. However, a disadvantage of this technique is that the internal solution resistance of the micropipet may limit the sensitivity of the measurement.

4.2.3. Imaging with Micropipet Ion-Selective Electrodes

In our work using the above-described distance-measuring techniques, different targets were imaged with different micropipet ion-selective electrodes. For imaging zinc concentration profiles, which can be important, e.g., in corrosion and microelectrode circuitry studies, a novel type of ionophore-based zinc micropipet ion-selective electrode was used. The zinc electrode was characterized on the basis of its calibration properties, selectivity, and response time. The selectivity studies carried out with the separate solution method [33] clearly showed that the incorporation of lipophilic anionic site additives in the ion-selective cocktail improved the ionophore-induced ion selectivity. In fact, in the absence of these mobile sites no zinc ion-selectivity is observed due to kinetic limitation of the ion transfer at the solution/membrane interface [34]. The most favorable ion-selectivity was observed using of 70 mol% KTpClPB relative to the ligand (Fig. 7). The zinc ion response of a zinc microelectrode in zinc nitrate solution also containing 5 mM tris(hydroxymethyl)aminomethane (pH7) is shown in Figure 8. These potentiometric data clearly demonstrate that the electrode function is almost theoretical, but also that the zinc ion sensitivity of the electrode is not affected by contact with $Ru(NH_3)_6Cl_3$ for different time intervals.

Different targets were imaged successfully with zinc SECM tips. In one of the experiments, steady-state zinc concentration profiles were created by ion migration generated with an electric current through a micro hole and by electrochemical reduction of zinc ions at the surface of a microdisk working electrode.

As described in Sect. 3.3., a-U-shaped target with a micropipet ending was prepared by filling it up with 0.1 M $Zn(NO_3)_2$ solution. In the measurement cell 0.1 NH_4Cl solution was added as a background electrolyte. By applying a dc voltage between two silver/silver chloride wires placed inside the cell and in the

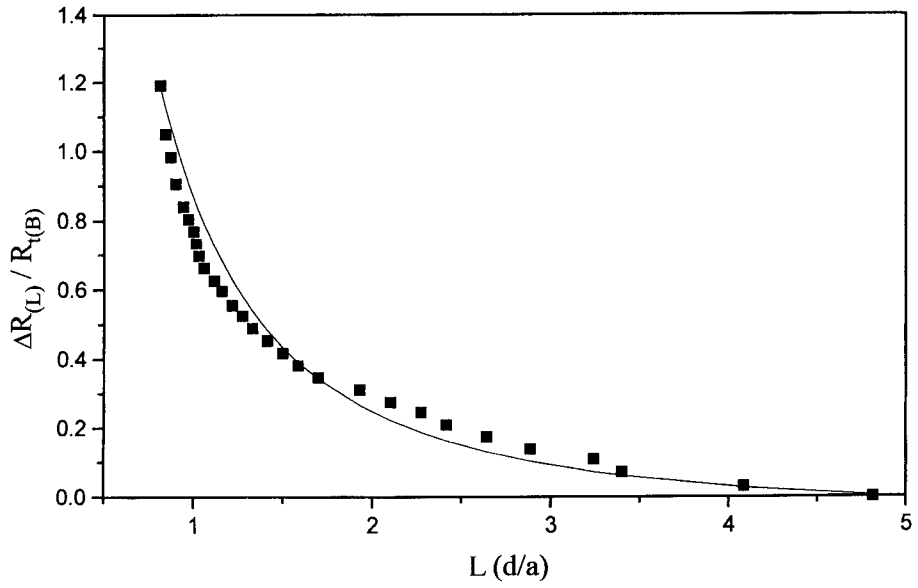

Fig. 6. Solution resistance curve for an Ag/AgCl micropipet electrode over a Teflon surface in 0.1 M KCl. Applied voltage: 50 mV; tip diameter: 20 μm. The squares are experimental data, while the line represents the theoretical data.

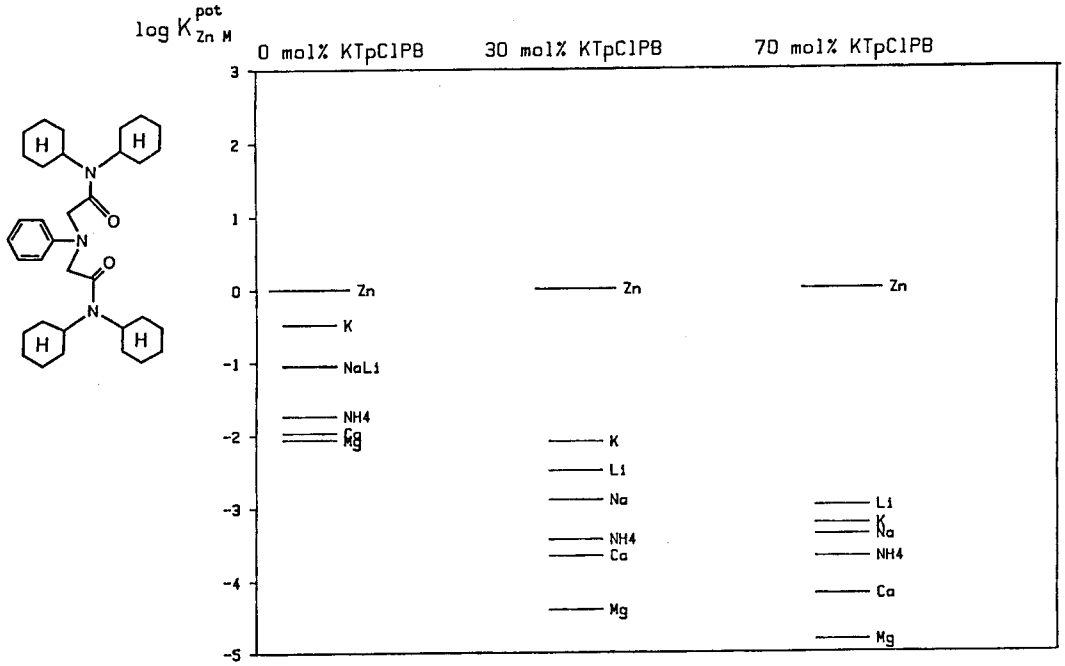

Fig. 7. Potentiometric selectivity coefficient of the zinc microelectrode with different mobile site concentrations. All data were determined by the separate solution method [34] at pH 7 (Tris-HCl buffer) with 0.1 M of the relevant chloride salts. Theoretical slope values were used for calculating the selectivity data.

noncapillary end of the target, an ion flux could be generated across the target micropipet opening. The polarity of the voltage was selected to drive the zinc ionic species from the target to the cell. After adjusting the tip–target distance, a constant dc potential was switched on, between the two wires and soon after, the potential imaging was performed.

Figure 9 shows a zinc concentration profile imaged over a 5-μm hole with a 9-μm zinc micropipet ion-selective electrode barrel. This result demonstrates that potentiometric SECM can be used for ion-selective imaging with relatively high resolution.

A microdisk target containing immobilized urease enzyme was prepared as described in Sect. 3.3. After mounting the target in the bottom of the measuring cell and roughly positioning the ammonium ion selective tip over the target, the tip–target distance was finely adjusted, as described previously [22]. A 0.1 M urea solution in Tris-buffer, pH7 was introduced into the cell and the potential of the NH_4^+ ion selective tip was followed. Owing to enzyme-catalyzed hydrolysis of the urea, the ammonium ion activity was high in the vicinity of the immobilized enzyme disk. In this way, the potentiometric SECM image of the target could be recorded. Figure 10 shows

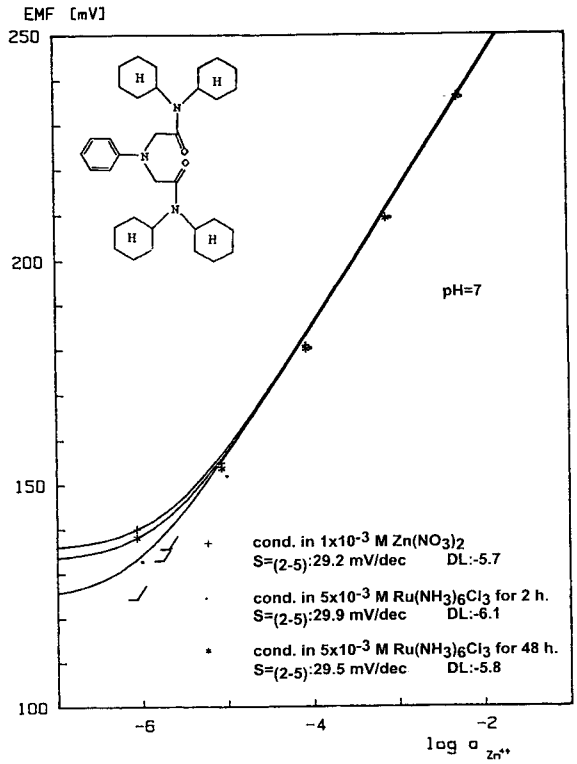

Fig. 8. Calibration properties of zinc microelectrodes in zinc nitrate solutions containing 5 mM Tris, pH 7 after conditioning them in solutions of different compositions. Tip diameter = 9 μm; the reference electrode was Ag/AgCl, 1 M KCl, 0.1 M CH_3COOLi. S: slope of the electrode calibration graph; DL: log of the detection limit.

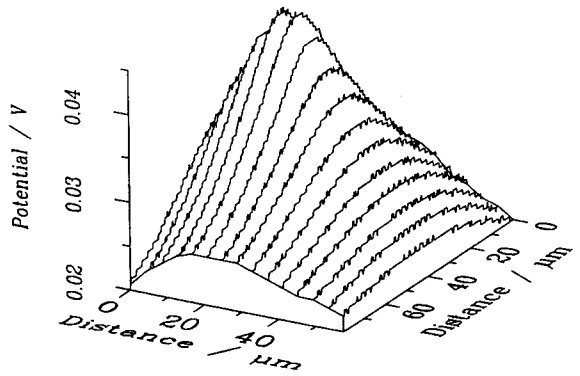

Fig. 9. Surface plot of the Zn^{2+} concentration profile around a Zn^{2+} source of a 9-μm diameter micropipet. Tip diameter = 15 μm; tip scan rate = 3 μm/s. The bulk solution concentrations inside and outside the micropipet were 0.1 M $Zn(NO_3)_2$ and 0.1 M NH_4Cl, respectively. Applied potential: 0.9 V.

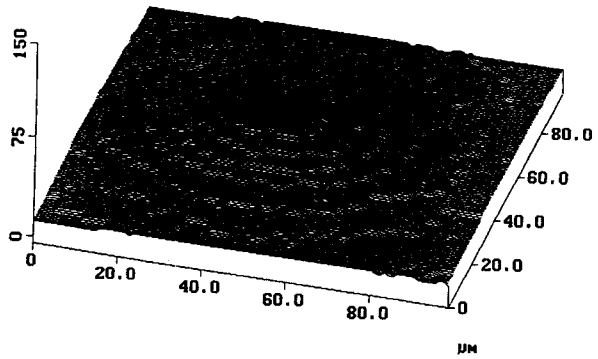

Fig. 10. Three-dimentional plot of the NH_4^+-concentration profile around a 20-μm diameter urease gel over the center of the target in 0.1 M urea and 0.1 M Tris-HCl buffer, pH 7. Tip diameter = 18 μm.

the three-dimensional plot for a concentration image of *a* ammonium ions over a 20-μm diameter urease disk target. The image was obtained at a constant height and the center of the target corresponds to the middle of the image. As can be seen, the concentration of ammonium ions was highest over the center of the target and decreased gradually in radial directions because of diffusion of the generated ammonium ions into the bulk solution.

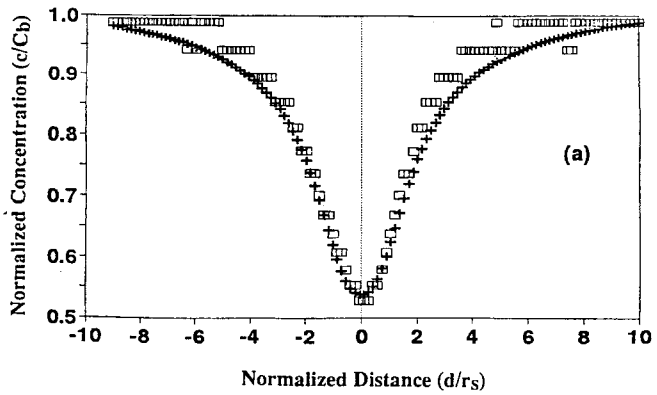

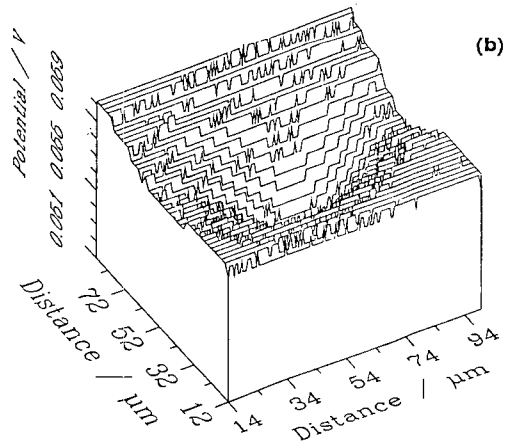

Fig. 11. Image of the Zn^{2+}-concentration profile around a 25-μm diameter Hg-coated Au electrode in 0.84 mM $Zn(NO_3)_2$ + 0.1 M NH_4Cl + 50 mM pH 7 Tris-HCl buffer: a) radial direction across the center of the electrode at a constant height of 11 μm from the surface. Electrode potential held at -1.15 V; tip diameter = 10 μm; tip scan rate = 2 μm/s. C_b: bulk concentration, r_s: target radius. Empty squares represent experimental data, while the pluses are the theoretical data: b) corresponding surface plot.

The results presented here clearly show that potentiometric probe microscopy with a micropipet ion-selective electrode can be used to map the distribution of enzyme activity on a surface. It must be mentioned that active urease enzyme spots cannot easily be noticed by amperometric SECM. The mapping of urease activity on surfaces using the local pH profile detected with the double function antimony microdisk electrode tip was reported earlier [22]. The major disadvantage in the use of a pH electrode for enzyme activity mapping is that it requires low buffer capacity solution media, which cannot be optimized for the enzyme catalytic reaction.

In the SECM experiments described above, the concentration of the species detected by the probe microscopy increased in the vicinity of the target surface. A reverse concentration profile was obtained by the electrochemical reduction of zinc ions on the surface of a mercury-coated gold microdisk electrode of 25-μm diameter. A 0.8 mM $Zn(NO_3)_2$ solution was employed containing 0.1 M NH_4Cl and 50 mM Tris-buffer adjusted to pH 7.0. The voltammograms showed that the plateau of Zn^{2+} reduction started around −1 V. In the SECM experiments a potential of −1.15 V vs. the Ag/AgCl reference was applied to the gold amalgam microelectrode target. In this way the evolution of hydrogen bubbles on the electrode and thus the concomitant disturbance of the concentration profile was avoided. An amperometric microelectrode used for measuring the Zn^{2+}-concentration can also perturb the concentration profile; thus the choice of a passive tip, i.e., the ion-selective zinc electrode, is more appropriate for imaging the surface concentration profile.

The precise determination of the position of the zinc-selective electrode barrel tip position in the Z direction was done with an open micropipet barrel. The concentration profile was also monitored by scanning in the $X-Y$ plane at a small distance from the surface, while the electrochemical reduction was proceeding. In this case, the lowest zinc ion concentration indicates the center of the amalgamated gold disk. Figure 11a shows the concentration profile across the center of the target recorded with a 10-μm zinc electrode at a constant (11 μm) distance from the surface, while Figure 11b exhibits the corresponding surface plot of the zinc image from above the mercury-coated gold target. The accumulation of zinc in the target could cause a decrease in the distance between the tip and the target. However, it was found that this effect was negligible within the time frame of the potentiometric imaging.

5. Conclusions

In this study three different electrochemical methods were compared for absolute calibration by measuring the tip–target distance. One of them, the earlier developed double function antimony microdisk electrode method is very simple, however, its applicability is limited to pH profiles. The use of two different approaches with double-barrel tips is more universal. The disadvantage of using the Ga microdisk barrel is that it requires an additional, external redox mediator. The micropipet distance sensor, on the other hand, is less sensitive.

The experimental results demonstrate that the imaging of local concentration profiles with passive, ion-selective measuring tips can be performed with high resolution. The main advantage of the potentiometric SECM is its applicability in determining the local concentration of electrochemically inert species. Due to this advantage, ion-selective SECM tips may

find many applications in experimental life science, in corrosion studies, and in investigations of heterogeneous chemical reactions. The applicability of a new ionophore-based zinc ultramicroelectrode as a measuring tip in SECM has been proven.

6. Acknowledgements

The authors express their gratitude to the National Science Foundation (CHE-8901450 and CHE-9214480), the Hungarian Academy of Sciences (Grant No: 45), and the Hungarian National Science Foundation (OTKA No.3115 & 3116).

7. References

[1] C. Lee, C.J. Miller, A.J. Bard, *Anal. Chem.* **1991,** *63*, 78.
[2] D. Ammann, *Ion Selective Microelectrodes: Principles, Design and Application*, Springer, New York **1986.**
[3] R.C. Thomas, *Ion Selective Intracellular Microelectrodes. How to make and use them*, Academic, London, **1978.**
[4] F.W. Orme, in *Glass Microelectrodes,* (Eds: M. Lavallée, O.F. Schanne, N.C. Herbert), Wiley, New York **1969,** pp. 376-395.
[5] Z. Stefanac, W. Simon, *Chimia* **1966,** *20*, 436.
[6] D. Amman,W.E. Morf, P. Anker, P.C. Meier, E. Pretsch, W.Simon, *Ion-Selective Electrodes Rev.* **1983,** *5*, 3.
[7] G. Binnig, H. Rohrer, *Helv. Phys. Acta* **1982,** *55*, 726.
[8] G. Binnig, H. Rohrer, C. Gerber, E. Weibel, *Phys. Rev. Lett.* **1983,** *50*, 120.
[9] R.C. Engström, M. Weber, D.J. Wunder, R. Burgess, S. Winquist, *Anal. Chem.* **1986,** *58*, 844.
[10] R.C. Engström, C.M. Pharr, *Anal. Chem.* **1989,** *61*, 1099A.
[11] A.J. Bard, F.-R.F. Fan, J. Kwak, O. Lev, *Anal. Chem.* **1989,** *61*, 132.
[12] J. Kwak, A.J. Bard, *Anal. Chem.* **1989,** *61*, 1221.
[13] A.J. Bard, M.V. Mirkin, P.R. Unwin, D.O. Wipf, *J. Phys. Chem.* **1992,** *96*, 1861.
[14] D.O Wipf, A.J. Bard, *Anal. Chem.* **1992,** *64*, 1362.
[15] J. Kwak, A.J. Bard, *Anal. Chem.* **1989,** *61*,1794.
[16] A.J. Bard, G. Denuault, C. Lee, D. Mandler, D.O. Wipf, *Acc. Chem. Res.* **1990,** *23*, 357.
[17] A.J. Bard, F.-R.F. Fan, D.T. Pierce, P.R. Unwin, D.O. Wipf, F. Zhou, *Science* **1991,** *245*, 68.
[18] D. Mandler, A. J. Bard, *J. Electrochem. Soc.* **1990,** *137*, 2468.
[19] A.J. Bard, R.-R.F. Fan, M.V. Mirkin, in *Electroanalytical Chemistry*, Vol. 18 (Ed: A. J. Bard), Marcel Dekker, New York **1994,** pp. 243-373.
[20] M. Arca, A.J. Bard, B.R. Horrocks, T.C. Richards, D.A. Treichel, *Analyst* **1994,** *119*, 719.
[21] G. Denault, M.H. Troise-Frank, L.M. Peter, *Faraday Discuss. Chem. Soc.* **1992,** *94*.
[22] B.R. Horrocks, M.V. Mirkin, D.T. Pierce, A.J. Bard, G. Nagy, K. Tóth, *Anal. Chem.* **1993,** *65*, 1213.
[23] C. Wei, A.J. Bard, G. Nagy, K. Tóth, *Anal. Chem.* **1995,** *67*, 1346.
[24] S. Glab, A. Hulanicki, G. Edwall, F. Ingman, *Crit. Rev. Anal. Chem.* **1989,** *21*, 29.
[25] H.A. Bicher, S. Ohki, *Biochim. Biophys. Acta* **1972,** *255*, 900.
[26] Y. Matsumura, K. Kajino, M. Fujimoto, *Membr. Biochem.* **1980,** *3*, 99.
[27] K. Tóth, G. Nagy, B.R. Horrocks, A.J. Bard, *Anal. Chim. Acta* **1993,** *282*, 239.
[28] G. Nagy, K. Tóth, C. Wei, A.J. Bard, unpublished.
[29] T.I. Popova, I.A. Bagodskaya, E.D. Moorhead, in *Encyclopedia of Electrochemistry of the Elements*, Vol. 8.(Ed: A.J. Bard), Marcel Dekker, New York **1978,** pp. 207-262.
[30] C.B. Prater, P.K. Hansma, *Rev. Sci. Instrum.* **1991,** *62*, 2634.
[31] P.K. Hansma, B. Drake, S.A.C. Gould, C.B. Prater, *Science* **1989,** *243*, 641.
[32] E. Lindner, M. Horváth, K. Tóth, E. Pungor, I. Bitter, B. Ágai, L. Töke, *Anal. Lett.* **1992,** *25*, 453.
[33] R. Eugster, P.M. Gehrig, W.E. Morf, U.E. Spichiger, W. Simon, *Anal. Chem.* **1991,** *63*, 2285.
[34] G.G. Guilbault, R.A. Durst, M.S. Frant, H. Freiser, E.H. Hansen, T.S. Light, E. Pungor, G. Rechnitz, N.M. Rice, T.J. Rohn, W. Simon, J.D.R. Thomas, *Pure Appl. Chem.* **1976,** *48*, 127.

Exploring Chaos & Complexity

Kaye, B.H.
Chaos & Complexity
Discovering the Surprising Patterns of Science and Technology
1993. XXII, 593 pages with 257 figures 2 in color and 43 tables.
Hardcover. DM 148.00.
ISBN 3-527-29039-7
Softcover: DM 78.00.
ISBN 3-527-29007-9

The surprising patterns of chaos and complexity are to be found in many areas of nature and science, examples ranging from cabbages to coastlines. Quite often, those who could benefit most from an understanding of the principles behind chaos and complexity, for example engineers, geologists, medics, chemists and physicists, are denied access to the power and wonders of the field by the mathematical and unnecessarily convoluted way the topic is usually presented.

This book opens up the fascinating opportunities offered by an understanding of this field to the informed layman, using informative and amusing examples of the application of the principles accompanied by many descriptive figures demonstrating the beauty of a science which can now be understood by all!

VCH, P.O. Box 10 11 61, D-69451 Weinheim, Telefax 06201-60 61 84 • VCH, Hardstrasse 10, P.O. Box, CH-4020 Basel • VCH, 8 Wellington Court, Cambridge CB1 1HZ, UK • VCH, 303 N.W. 12th Avenue, Deerfield Beach, FL 33442-1788, USA (toll-free: 1-800-367-8249) • VCH, Eikow Building, 10-9 Hongo 1-chome, Bunkyo-ku, Tokyo 113

VCH